ELSEVIER

Journal of Nuclear Materials 283–287 (2000) 391–395

journal of nuclear materials

www.elsevier.nl/locate/jnucmat

Irradiation creep at 60°C in SUS 316 and its impact on fatigue fracture

Johsei Nagakawa [a,b,*], Y. Murase [a], N. Yamamoto [a], T. Fukuzawa [a]

[a] Advanced Nuclear Materials Division, National Research Institute for Metals, 1-2-1 Sengen, Tsukuba, Ibaraki 305-0047, Japan

[b] Advanced Energy Engineering Science, Interdisciplinary Graduate School of Engineering Sciences, Kyushu University, 6-1 Kasuga Koen, Kasuga, Fukuoka 816-8580, Japan

Abstract

Structural materials in fusion reactors will be subjected to irradiation by energetic particles at temperatures widely ranging from liquid He to above 1000°C. Hence, the very large irradiation creep strain at 60°C previously reported in the ORR/ORNL pressurized tube experiment to 8 dpa is important. Computer calculations for the 20% cold-worked SUS 316 demonstrated the transient nature of this radiation-induced creep, caused by the overwhelming flux of excess interstitial atoms lasting nearly one year at 60°C where the diffusivity of vacancies is very low. In order to confirm such a transient nature, continuous creep measurement under irradiation is necessary and was carried out using 17 MeV protons. Development of very significant creep strain, much larger than that at 300°C, and steadily decreasing creep rate were observed at 60°C as the calculation predicted. A significant influence of the dynamic irradiation effect at 60°C on fatigue fracture was also observed.

1. Introduction

Structural materials in fusion reactors will be subjected to irradiation by energetic particles at temperatures widely ranging from liquid He to above 1000°C. Accumulation of a large creep strain was observed at 60°C in the pressurized tube experiments of austenitic stainless steels irradiated to about 8 dpa in the ORR/ORR [1]. The observed strain was several times larger than that at 300–400°C, which was already larger by orders of magnitude than that of thermally activated creep. Although the major components of the fusion reactors will be irradiated at rather high temperatures, there will be many portions which suffer from atomic displacements and stress at lower temperatures.

At around 60°C, vacancies can hardly move in the austenitic stainless steels due to their high migration energy [2]. Since the radiation-induced deformation is caused mainly by the motion of interstitial atoms, the large difference in diffusivity may lead to a very significant enhancement. In this study, a calculational investigation was first performed for 20% cold-worked SUS 316 stainless steel at both 60°C and 300°C. Second, continuous measurements of creep strain during 17 MeV proton irradiation were carried out at 300°C and 60°C. Since the earlier results at the ORR/ORNL were not obtained as a function of irradiation time, those data are inadequate to provide a thorough verification of the theoretical conclusions. Third, the impact of such enhanced dynamic irradiation effect at 60°C on fatigue fracture was also examined.

2. Modeling and calculation procedure

The present simulation is based on the stress-affected kinetics of radiation-induced defects. Simultaneous differential equations are numerically solved for the following defect concentrations [3]: C_i, single interstitials; C_v, single vacancies; C_{2iA}, aligned interstitial loop precursors; C_{2iN}, non-aligned interstitial loop precursors; C_{ilA}, growing interstitial loops on aligned planes; C_{ilN}, those on non-aligned planes; C_{ilAi}, accumulated net interstitials in growing aligned loops; C_{ilNi}, those in growing non-aligned loops; C_{dAi}, net interstitials

* Corresponding author. Tel.: +81-298 59 2014; fax: +81-298 59 2014.

E-mail address: johsei@nrim.go.jp (J. Nagakawa).

0022-3115/00/$ - see front matter
PII: S0022-3115(00)00078-7

absorbed by aligned network dislocations; C_{dNi}, those absorbed by non-aligned network dislocations.

Point defect migration energies for SUS 316 stainless steel were taken from the evaluation by Dimitrov and Dimitrov [2], that is, 0.92 eV for interstitials and 1.15 eV for vacancies. This rather high migration energy of interstitials in austenitic stainless steels was supported by studies of microstructural evolution [4]. The same parameter values as in [3] were used. The interstitial absorption bias (Z_i) and its stress-induced component (ΔZ_i) for loops and network dislocations were calculated using the equations given by Wolfer and Ashkin [5,6] and Heald and Speight [7], respectively. As for a vacancy flux, values for Z_v and ΔZ_v given by [5–7] were used in the calculation. At each numerical iteration step, the loop size was re-averaged and $Z_{i,v}$ and $\Delta Z_{i,v}$ were re-evaluated. In the interstitial loop nucleation process, a di-interstitial was taken to be a precursor and its formation was considered to be affected by the external stress following the SIPN model proposed by Brailsford and Bullough [8].

In the present study, stress-induced preferential nucleation of interstitial loops (SIPN) [8,9] and loop growth driven by stress-induced preferred absorption of point defects (SIPA) [7,10] are taken into account, as well as SIPA climb (PA) and glide enabled by SIPA climb (PAG) contributions [11] by network dislocations. Also included was transient mode of I-creep (TIC) [12]; dislocation glide enabled by the enhanced climb motion due to the excess interstitial flux during the transient stage of point defect kinetics) [13,14]. The plastic strain rate produced by each mechanism was evaluated at every iteration step using the following equations;

(1) PA

$$\dot{\varepsilon}_{PA} = \frac{2}{3}(dC_{dAi}/dt - dC_{dNi}/dt). \tag{1}$$

(2) PAG

$$\dot{\varepsilon}_{PAG} = \left(4e\sqrt{(\pi L_d)}/3b)(dC_{dAi}/dt - dC_{dNi}/dt\right). \tag{2}$$

(3) SAIL (SIPA climb creep by growing interstitial loops) [7,10]

$$\dot{\varepsilon}_{SAIL} = \frac{2}{3}(dC_{ilAi}/dt - dC_{ilNi}/dt). \tag{3}$$

(4) SIPN

$$\dot{\varepsilon}_{SIPN} = \frac{4}{3}(dC_{2iA}/dt - dC_{2iN}/dt). \tag{4}$$

(5) TIC

$$\dot{\varepsilon}_{TIC} = \left(e\sqrt{(\pi L_d)}/b\right)(dC_{dAi}/dt + 2dC_{dNi}/dt), \tag{5}$$

where e is the elastic deflection (σ/E; σ is the external stress, E is Young's modulus), L_d is the network dislocation density, and b is the size of the Burgers vector. The damage efficiency for light-ion irradiation was set to unity, which resulted in a good coincidence with the experiments, including temperature dependence [3].

3. Experimental procedure

Continuous irradiation creep measurement at 60°C were performed using the in-beam creep-fatigue testing apparatus connected to the NRIM compact cyclotron accelerator [15,16]. The tested material was SUS 316 (Cr: 16.79, Ni: 10.30, Mn: 1.17, Mo: 2.16, C: 0.06, Si: 0.68, P: 0.027, S: 0.001, Fe: balance, in wt%), with a grain size of less than 10 μm and cold-worked to 20%. The specimen was in a thin sheet shape with a gauge section 4 mm wide, 10 mm long and 150 μm thick. The 17 MeV proton beam with an intensity of 2 μA/cm^2 produces atomic displacements at a rate of about 1×10^{-7} dpa/s ±5.5% throughout the 150 μm thick specimen set at 45° to the incident beam. The torsional creep apparatus and a 20% cold-worked thin wire specimen 125 μm in diameter [17] was used for the 300°C experiment. This was because the irradiation creep rate at 300°C was too small for the creep-fatigue apparatus. Previous results demonstrated that there was only a small difference between the two types of testing [3]. The specimen temperature was controlled by balancing the beam heating and the He jet cooling for 60°C, while a heated He jet was used for 300°C.

In-beam fatigue behavior was examined under 17 MeV proton irradiation at 60°C in a load-controlled tension–tension mode using the apparatus mentioned above. A side-notch 0.12 mm wide, 0.60 mm long with a notch-tip radius of 0.06 mm at the center was made by the spark erosion method to the fatigue specimens of the same size as the creep specimens [16].

4. Results and discussion

Fig. 1 shows the calculated irradiation creep rate as a function of time at 300 MPa for 60°C and 300°C with 10^{-7} dpa/s in the 20% cold-worked SUS 316. The major contributing mechanism at 60°C is SIPN, and TIG is the second most important. At 300°C PA contributes most, followed by TIC and PAG. The large peaks, which reflect the transient excess interstitial flux, disappear as the density of vacancies in the matrix increases and the mutual recombination of point defects becomes significant. Ultimately a steady state creep rate will be attained, but it is much delayed at 60°C, nearly one year, presenting a striking contrast to the order of seconds at 300°C. The calculated steady-state creep rate is not so different between 300°C (1.95×10^{-10} s^{-1}) and 60°C (1.05×10^{-10} s^{-1}). The calculation also gives the creep

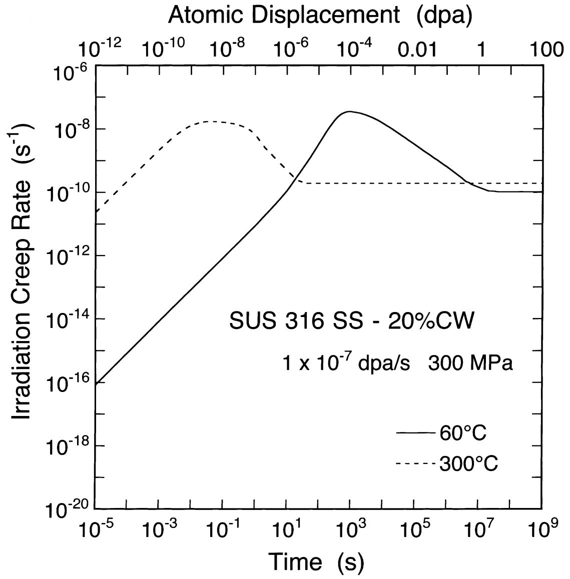

Fig. 1. Calculated irradiation creep rate vs time at 60°C and 300°C.

strain development with irradiation time, shown in Fig. 2. A clear and significant transient behavior with a gradually decreasing creep rate can be recognized at 60°C. At 60°C the creep rate at 5–6 $\times$ 10^4 s is about 5 $\times$ 10^{-9} s^{-1}, which is higher than that at 300°C by about 20 times.

Continuous measurements were performed under 17 MeV proton irradiation. Fig. 3 indicates the results for

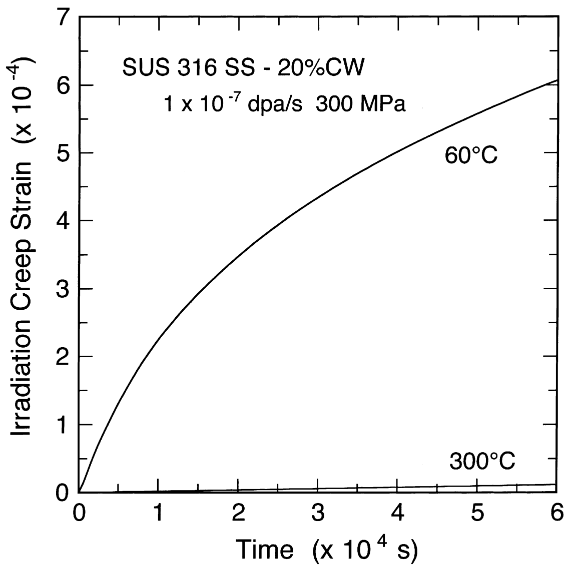

Fig. 2. Calculated irradiation creep strain vs time at 60°C and 300°C.

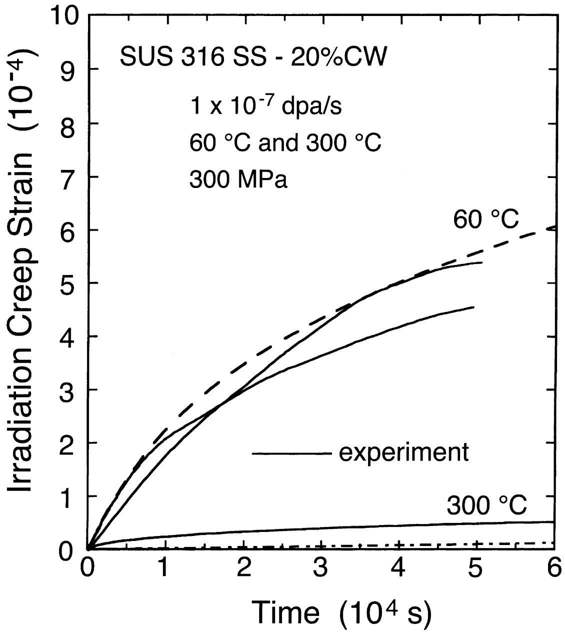

Fig. 3. Comparison of the creep curves between calculation and experiment at 60°C and 300°C.

both 60°C and 300°C. At 300°C a weak but rather prolonged transient stage can be seen. As shown in Fig. 4, the transient is almost finished at about 6 $\times$ 10^4 s and reaches close to the calculated value of 1.95 $\times$ 10^{-10} s^{-1}. The main cause of this 300°C transient seems to be associated with thermal recovery, possibly assisted by the irradiation, of the cold-worked dislocation structure, although the exact origin is not clear at

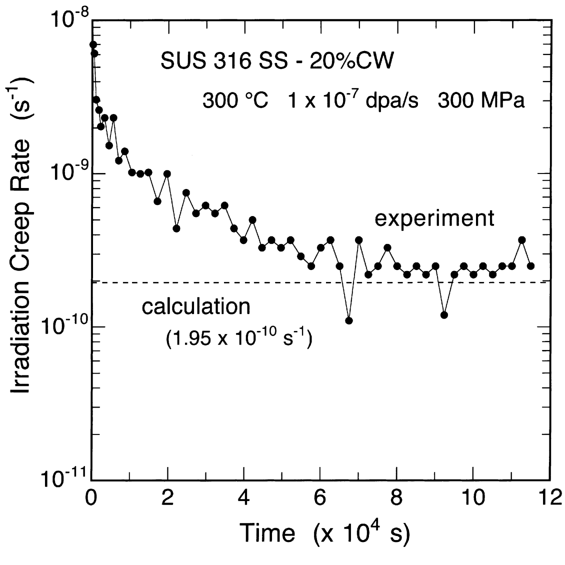

Fig. 4. Creep rate change with time under irradiation at 300°C.

this moment. The transient at 60°C is far more significant, and the creep rate at 5×10^4 s is higher than that at 300°C by more than one order of magnitude and still decreasing steadily. As shown in Fig. 5, correspondence of the creep rate change between the experimental and the calculational results at 60°C appears to be fairly good. These calculated and experimental results strongly suggest that the low temperature irradiation creep at 60°C in SUS 316 originates in the transient of irradiation-induced point defects caused by their large difference in diffusivity.

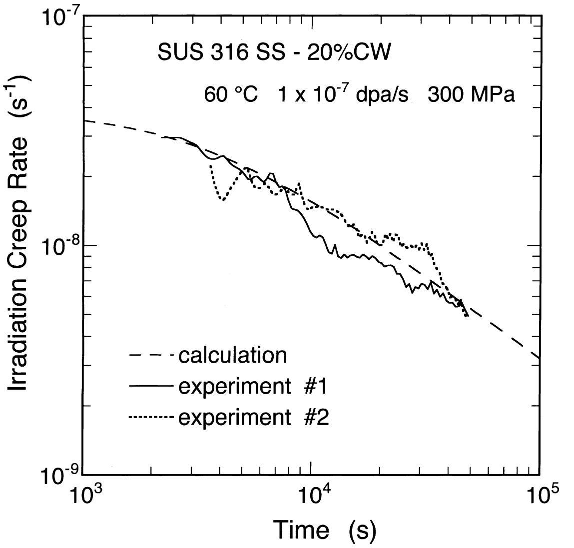

Fig. 5. Comparison of the irradiation creep rate change with time between experiment and calculation at 60°C.

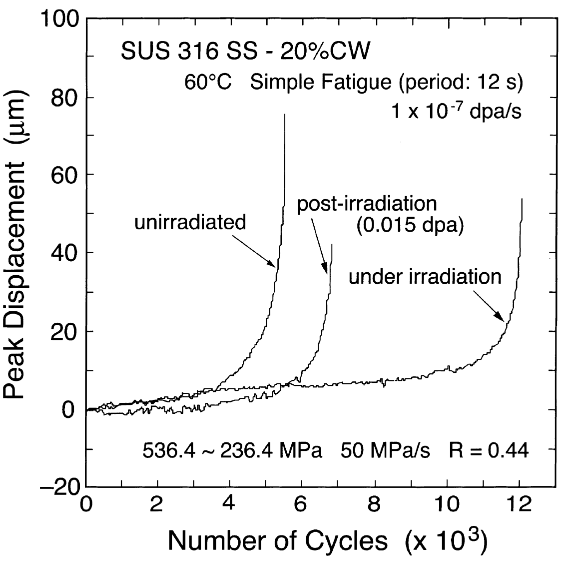

Fig. 6. Displacement at the maximum load vs the number of cycles for fatigue tests at 60°C.

Influence of the dynamic effect of irradiation at 60°C on fatigue behavior was examined under 17 MeV proton irradiation in a load-controlled tension–tension mode. Fig. 6 shows the axial displacement at the maximum load relative to that at the first cycle as a function of the number of cycles. Each test was duplicated and the result was similar in each case. The applied maximum load corresponds to 90% of the yield stress at the notched ligament. It can be seen that the fatigue life is considerably extended compared with that for the unirradiated case. This extended life is not due to a simple irradiation hardening, because a specimen pre-irradiated to 0.015 dpa, i.e., the total accumulated damage in the fractured in-beam specimen, showed a much smaller prolongation in a post-irradiation test. Hence, the large life extension under irradiation may be primarily due to a significant dynamic irradiation effect at 60°C.

5. Conclusions

Creep deformation and fatigue fracture in SUS 316 – 20% CW under 17 MeV proton irradiation at 60°C were investigated.

1. Calculation has shown that the large radiation-induced creep at 60°C is a transient phenomenon and it originates from the difference in diffusivity between vacancy and interstitial at this temperature.
2. In confirmation, continuous creep measurements were carried out under 17 MeV proton irradiation at 1×10^{-7} dpa/s, 60°C and 300°C. Very significant creep strain, much larger than that at 300°C, and steadily decreasing creep rate were observed at 60°C as the calculation predicted.
3. Load-controlled fatigue life of side-notched specimens was prolonged considerably under irradiation, while much less after irradiation at 60°C. This indicates that life extension was not due to a simple irradiation hardening but it may result from a dynamic irradiation effect.

References

[1] M.L. Grossbeck, L.K. Mansur, J. Nucl. Mater. 179–181 (1991) 130.
[2] C. Dimitrov, O. Dimitrov, J. Phys. F 14 (1984) 793.
[3] J. Nagakawa, N. Yamamoto, H. Shiraishi, J. Nucl. Mater. 179–181 (1991) 986.
[4] N. Yoshida, J. Nucl. Mater. 205 (1993) 344.
[5] W.G. Wolfer, M. Ashkin, J. Appl. Phys. 46 (1975) 547.
[6] W.G. Wolfer, M. Ashkin, J. Appl. Phys. 46 (1975) 4108.
[7] P.T. Heald, M.V. Speight, Philos. Mag. 29 (1974) 1075.
[8] A.D. Brailsford, R. Bullough, Philos. Mag. 27 (1973) 49.

[9] R.V. Hesketh, Philos. Mag. 7 (1962) 1417.
[10] R. Bullough, J.R. Willis, Philos. Mag. 31 (1975) 855.
[11] L.K. Mansur, Philos. Mag. A 39 (1079) 497.
[12] J.H. Gittus, Philos. Mag. 25 (1972) 345.
[13] R.E. Stoller, M.L. Grossbeck, L.K. Mansur, in: R.E. Stoller, A.S. Kumar, D.S. Gelles (Eds.), ASTM STP 1125, ASTM, Philadelphia, 1992, p. 517.
[14] J. Nagakawa, J. Nucl. Mater. 225 (1995) 1.
[15] J. Nagakawa, Y. Murase, N. Yamamoto, in: Proceedings of the IEA/JUPITER Joint Symposium on Small Specimen Technology for Fusion Research, 1999, in press.
[16] Y. Murase, J. Nagakawa, N. Yamamoto, Y. Fukuzawa, ASTM STP 1366, ASTM, Philadelphia, 2000, p. 713.
[17] J. Nagakawa et al., J. Nucl. Mater. 136 (1985) 238.